

Electronic Supplementary Information (ESI)

Tungsten trioxide nanoplate array supported platinum as highly efficient counter electrode for dye-sensitized solar cells

Dandan Song,^a Peng Cui,^a Xing Zhao,^a Meicheng Li,^{a,b*} Lihua Chu,^a Tianyue Wang^a and Bing Jiang^a

^a State Key Laboratory of Alternate Electrical Power System with Renewable Energy Sources, School of Renewable Energy, North China Electric Power University, Beijing 102206, China.

^b Chongqing Materials Research Institute, Chongqing 400707, China.

* Corresponding author information: E-mail: mcli@ncepu.edu.cn; Fax: +86 10 6177 2951; Tel: +86 10 6177 2951.

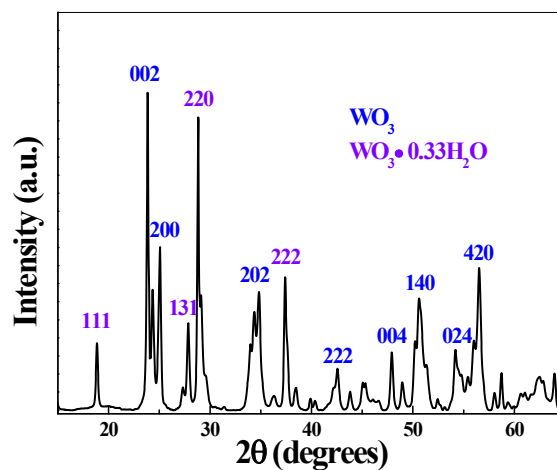


Fig. S1 XRD pattern of hydrothermally fabricated WO₃ on FTO/glass substrate

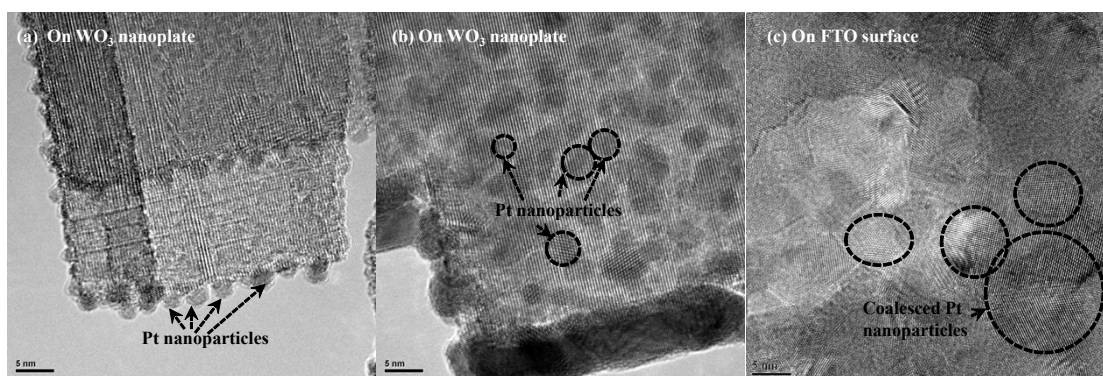


Fig. S2 High resolution transmission electron microscopy (HRTEM) images from Pt (3 nm)/WO₃ sample (a, b) and Pt (3 nm)/FTO sample (c). The arrows in (a, b) point to several representative Pt nanoparticles, which have diameters in the range of 2-5 nm. It can be seen that the Pt nanoparticles distributes discretely on the edge and surface of WO₃ nanoplate. The coalesced Pt nanoparticles can be observed in Pt (3 nm)/FTO sample (c). The formation of discrete Pt nanoparticles on WO₃ nanoplate favors the charge transfer between Pt and triiodide, which will result in the high catalytic activity of Pt/WO₃ counter electrode.

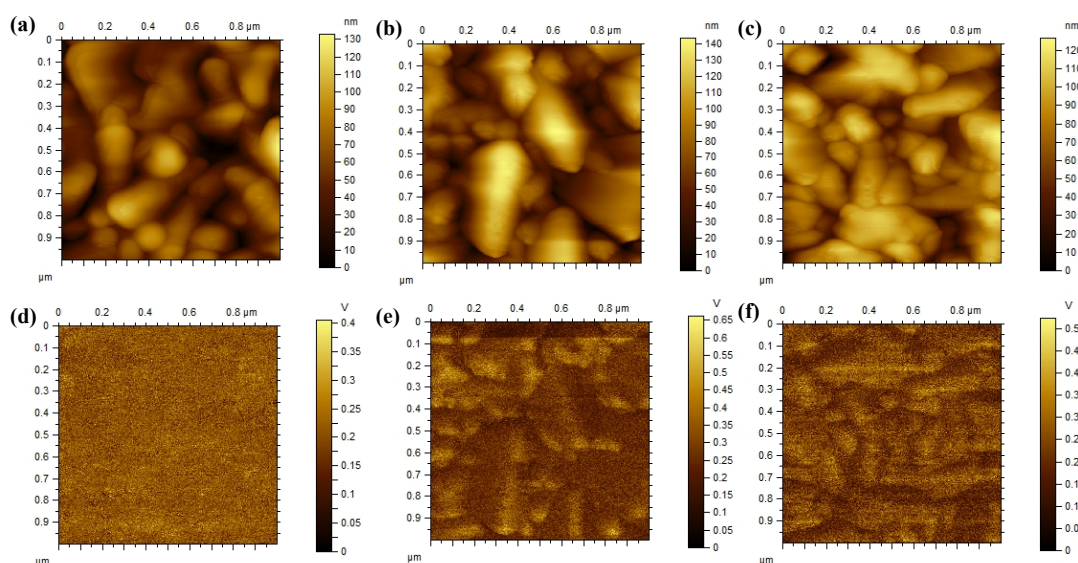


Fig. S2 Atomic force microscope (AFM) images and kelvin potential microscope (KPFM) images of FTO (a and d), Pt (1 nm)/FTO (b and e) and Pt (3 nm)/FTO (c and f), respectively. Pt nanoparticles are hard to be observed in AFM images shown in Fig. S1b and 1c due to the small sizes. However, in KPFM images, they can be clearly identified due to the different electronic properties of Pt and FTO background. Pt nanoparticles show higher local surface potential (corresponding to the bright color) than FTO, and it can be clearly seen that the amount of Pt

nanoparticles increases with the nominal thickness of Pt film. It also shows that Pt nanoparticles distribute heterogeneously on FTO surface.

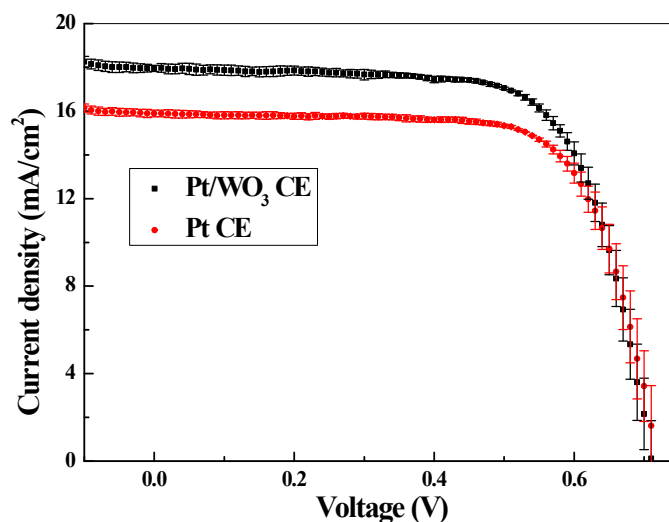


Fig. S5. J-V curves with error bars of DSCs using Pt and Pt/WO₃ nanoplate array CEs. The error bars are plotted according to the standard deviation of the J-V curves obtained from multiple cells.

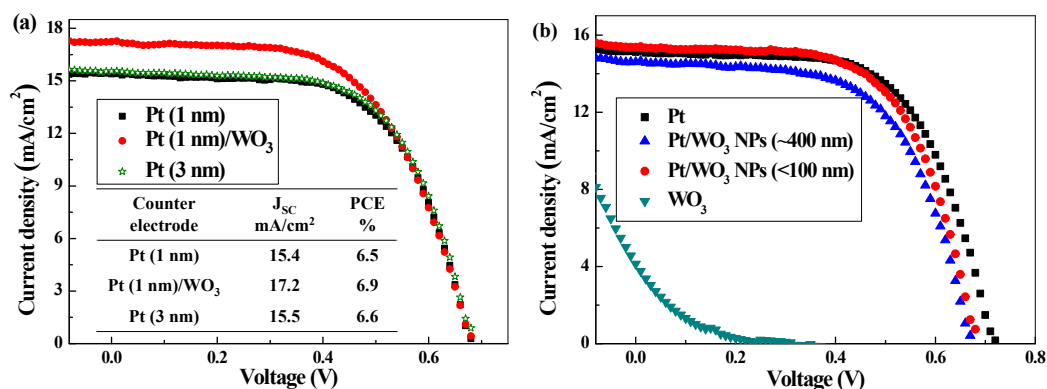


Fig. S5. J-V curves of DSCs (a) using Pt with different thickness and Pt/WO₃ nanoplate array CEs, and (b) using Pt (2 nm)/WO₃ nanoparticles (NPs) and pristine WO₃ CEs. The films composed of WO₃ nanoparticles (50 nm in diameter) were obtained by spin-coating of WO₃ slurry on FTO/glass substrates. Their thickness was controlled by varying the spin-coating speed and measured by a step profiler.

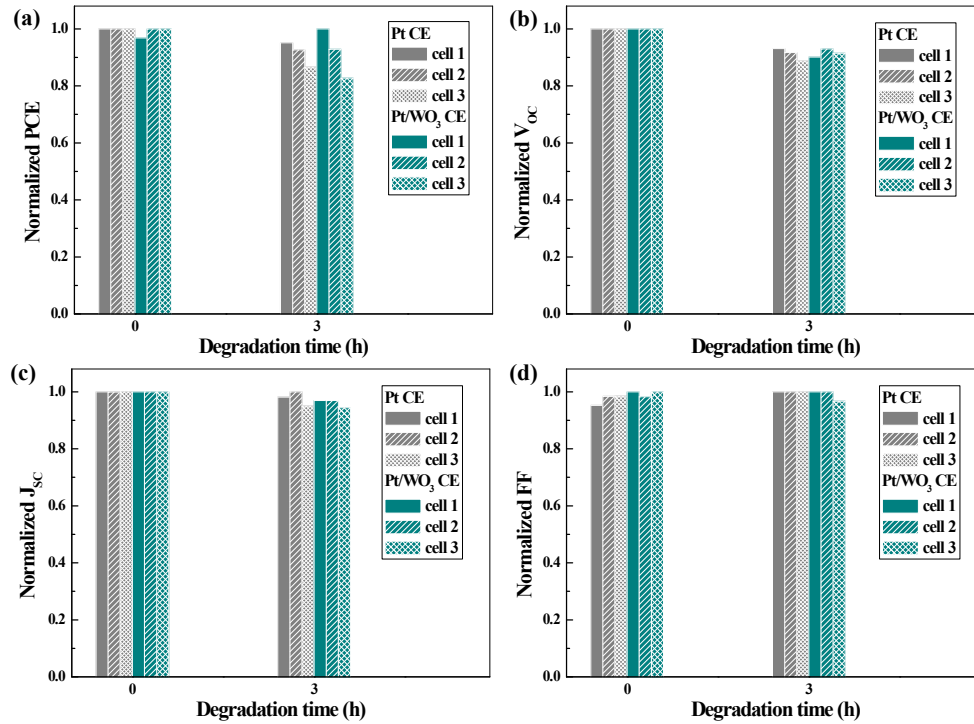


Fig. S6 The photovoltaic parameters of the DSCs using Pt CE and Pt/WO₃ CE before and after degradation at 80 °C. The photovoltaic performance of the cells was measured under an irradiation of 100 mW/cm². It can be seen that the degradation in PCE is mainly caused by the decreased V_{OC} . In theory, the V_{OC} is determined by the potential difference between the photoanode and the electrolyte. Therefore, the change in the CE materials plays minor effect on the V_{OC} and the stability of the DSCs. Hence, though the presence of WO₃ in the CE probably accelerates the Pt dissolution via the increased the surface area with the fine Pt nanoparticles, it has minor effect on the stability of the DSCs.